

Hierarchically mesoporous carbon nanopetal based electrodes for flexible supercapacitors with super-long cyclic stability

Jayesh Cherusseri^a and Kamal K. Kar^{a,b*}

^aAdvanced Nanoengineering Materials Laboratory, Materials Science Programme, Indian Institute of Technology, Kanpur, Uttar Pradesh-208016, India.

^bAdvanced Nanoengineering Materials Laboratory Department of Mechanical Engineering, Indian Institute of Technology, Kanpur, Uttar Pradesh-208016, India.

*Corresponding Author. Tel: +91-512-2597687, E-mail: kamalkk@iitk.ac.in (Kamal K. Kar)

Electronic Supplementary Information

List of Contents

Supplementary Tables:

Table S1. Comparison of gravimetric capacitances achieved by the various carbon nanomaterials based supercapacitors.

Supplementary Methods:

Method S1. Calculation of ionic conductivity of CNPs/UCF supercapacitor electrodes.

Method S2. Calculation of discharge capacitance of CNPs/UCF supercapacitor.

Method S3. Calculation of areal capacitance of CNPs/UCF supercapacitor.

Method S4. Calculation of volumetric capacitance of CNPs/UCF supercapacitor.

Method S5. Calculation of volume specific capacitance of CNPs/UCF supercapacitor

Method S6. Calculation of volume specific energy density of CNPs/UCF supercapacitor.

Method S7. Calculation of volume specific power density of CNPs/UCF supercapacitor.

Method S8. Calculation of gravimetric capacitance of CNPs/UCF supercapacitor.

Method S9: Calculation of gravimetric energy density of CNPs/UCF supercapacitor.

Supplementary Figures:

Fig. S1. Assembly of CNPs/UCF supercapacitor cell by using CNPs/UCF electrode-cum-current collectors.

Fig. S2. SEM image of nickel-coated UCFs.

Fig. S3. EDS spectra of oxidized, nickel-coated UCFs.

Fig. S4. Plot of variations in the volumetric capacitance of CNPs/UCF supercapacitor cell at different current densities.

Fig. S5. Digital image of the two electrode cell set-up used for the testing of CNPs/UCF supercapacitor at various bending angles.

Fig. S6. Plot of percentage retention in the areal capacitance of CNPs/UCF supercapacitor cell at different bending angles.

Fig. S7. Plot of percentage retention in the gravimetric capacitance of CNPs/UCF supercapacitor cell at different bending angles.

Fig. S8. Plot of variation in the volumetric capacitance of CNPs/UCF supercapacitor cell at different bending angles.

Fig. S9. Plots of percentage retentions in the volumetric and volume specific capacitances of CNPs/UCF supercapacitor cell at different bending angles.

Fig. S10. Plot of variation in the gravimetric energy density of CNPs/UCF supercapacitor cell at different bending angles.

Fig. S11. Plots of percentage retentions in the volume specific and gravimetric energy densities of CNPs/UCF supercapacitor cell at different bending angles.

Fig. S12. Plots of percentage retentions in the volume specific and gravimetric power densities of CNPs/UCF supercapacitor cell at different bending angles.

Table S1. Comparison of gravimetric capacitances achieved by the various carbon nanomaterials based supercapacitors.

Ref.	Electrode Material/s	Electrolyte	$C_{sc,sp,m}$ (F/g)
[S2]	SWNTs	1 M NaCl (aqueous)	25-30
	MWNTs	1 M NaCl (aqueous)	6-10
[S3]	MWNTs	1 M LiPF ₆ (EC-DEC)	35
[S4]	Normal CNTs	1 M LiClO ₄ (EC-DEC)	25
	Activated CNTs	1 M LiClO ₄ (EC-DEC)	50
[S5]	CO ₂ -oxidized CNTs	--	47
[S6]	MWNTs	6 N KOH	21
[S7]	MWNTs	1 M H ₂ SO ₄	25.4
[S8]	SWNTs	6 M KOH	40
[S9]	Pristine CNTs	Aprotic electrolyte	12.9
	Pristine CNTs	Protic electrolyte	10.9
	Cup-stacked CNTs	Aprotic electrolyte	55.7
	Cup-stacked CNTs	Protic electrolyte	28.4
[S10]	Pristine DWNTs	0.5 M H ₂ SO ₄	22
	Pristine DWNTs	1 M Et ₄ NBF ₄ /PC	34
	DWNT-HNO ₃	0.5 M H ₂ SO ₄	54
	DWNT-HNO ₃	1 M Et ₄ NBF ₄ /PC	38
[S11]	MWNTs grown on metals	6 M KOH	10.75-21.57
[S12]	CNTs grown on Ni-foam	6 M KOH	25
[S13]	SWNT film	1 M LiClO ₄ (EC-DEC-DMC)	35
[S14]	MWNTs	38 wt% H ₂ SO ₄	113
[S15]	SWNTs	7.5 N KOH	180

Present Work	CNPs synthesized on UCF	5 M KOH	220 (at 2.77mA/cm²) 154 (at 16.66mA/cm²)
---------------------	--------------------------------	----------------	---

Method S1. Calculation of ionic conductivity of CNPs/UCF electrodes.

The ionic conductivity of the supercapacitor electrodes is calculated by using the equation

$$\sigma = \frac{T}{R_b \times A}$$

Where σ is the ionic conductivity in S/cm, T is the total thickness of the supercapacitor cell (in cm), R_b is the bulk electrolyte resistance (in Ω), and A is the geometrical area of electrodes (in cm^2).

Method S2: Calculation of discharge capacitance of CNPs/UCF supercapacitor.

The discharge capacitance of the supercapacitor is calculated by using equation

$$C_{sc} = \frac{It_{dis}}{\Delta E}$$

Where, C_{sc} is the discharge capacitance of the supercapacitor, I is the charging current, t_{dis} is the discharging time, and ΔE is the operating potential window.

Method S3: Calculation of areal capacitance of CNPs/UCF supercapacitor.

The areal capacitance of the supercapacitor is calculated by using the equation

$$C_{sc, A} = \frac{C_{sc}}{A_{sc}}$$

Where, $C_{sc, A}$ is the areal capacitance of the supercapacitor and A_{sc} is the total geometric area of two supercapacitor electrodes (i.e., two times the area of single electrode).

Method S4: Calculation of volumetric capacitance of CNPs/UCF supercapacitor.

The volumetric capacitance of the supercapacitor is calculated by using the equation

$$C_{sc, V} = \frac{C_{sc}}{V_{sc}}$$

Where, $C_{sc,V}$ is the volumetric capacitance of the supercapacitor and V_{sc} is the total volume of the supercapacitor (total volume of two supercapacitor electrodes + volume of the separator with electrolyte).

Method S5: Calculation of volume specific capacitance of CNPs/UCF supercapacitor.

The volume specific capacitance of the supercapacitor is calculated [S1] by using the equation

$$C_{sc, sp, V} = 4 \times \frac{C_{sc}}{V_{el}}$$

Where, $C_{sc,sp,V}$ is the volume specific capacitance of the supercapacitor, C_{sc} is the discharge capacitance of the supercapacitor, V_{el} is the total volume of two supercapacitor electrodes (the volumes of separator with electrolyte is not considered).

Method S6: Calculation of volume specific energy density of CNPs/UCF supercapacitor.

The volume specific energy density of the supercapacitor is calculated by using the equation

$$E_{sc, sp, V} = \frac{C_{sc, sp, V} \times (\Delta E)^2}{2 \times 3600}$$

Where $E_{sc,sp,V}$ is the volume specific energy density and all other variables as defined above.

Method S7: Calculation of volume specific power density of CNPs/UCF supercapacitor.

The volume specific power density of the supercapacitor is calculated by using the equation

$$P_{sc, sp, V} = \frac{E_{sc, sp, V} \times 3600}{t_{dis}}$$

Where $P_{sc,sp,V}$ is the volume specific power density and all other variables are defined above.

Method S8: Calculation of gravimetric capacitance of CNPs/UCF supercapacitor.

The gravimetric capacitance of the supercapacitor is calculated by using the equation

$$C_{sc,sp,m} = \frac{I \times t_{dis}}{M \times (\Delta E)} = \frac{C_{sc}}{M}$$

Where, ‘M’ is the total mass of CNPs in the two electrodes of the supercapacitor (excluding the mass of UCFs, separator, and electrolyte), and other variables are discussed above.

Method S9: Calculation of gravimetric energy density of CNPs/UCF supercapacitor.

The gravimetric energy density of the supercapacitor is calculated by using the equation

$$E_{sc, sp, m} = \frac{C_{sc, sp, m} \times (\Delta E)^2}{2 \times 3600}$$

Where $E_{sc, sp, m}$ is the gravimetric energy density and all other variables are defined above.

Supplementary Figures:

Fig. S1. Assembly of CNPs/UCF supercapacitor cell by using CNPs/UCF electrode-cum-current collectors.

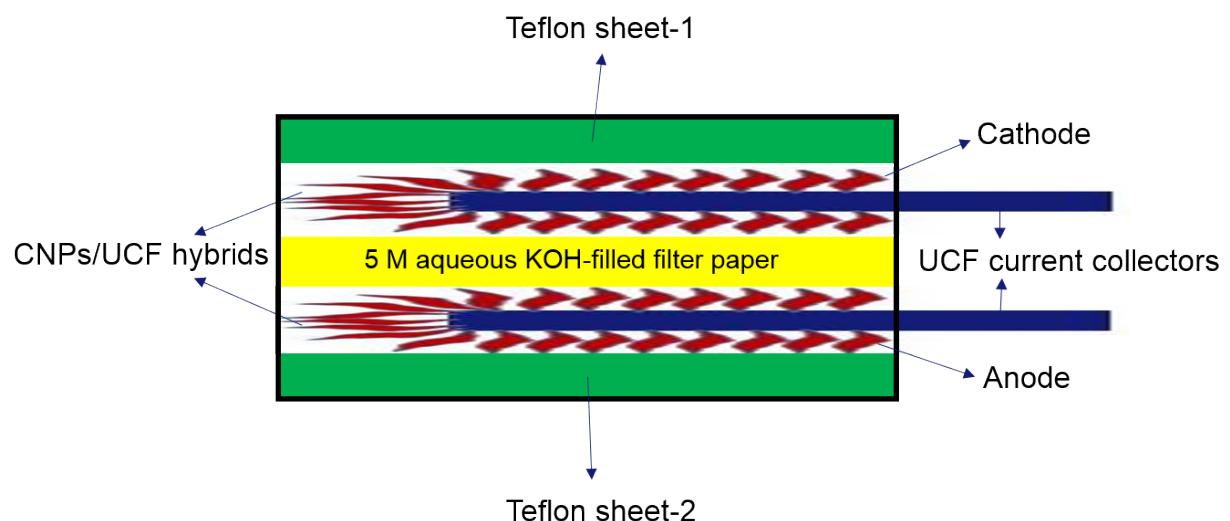


Fig. S2. SEM image of nickel-coated UCFs.

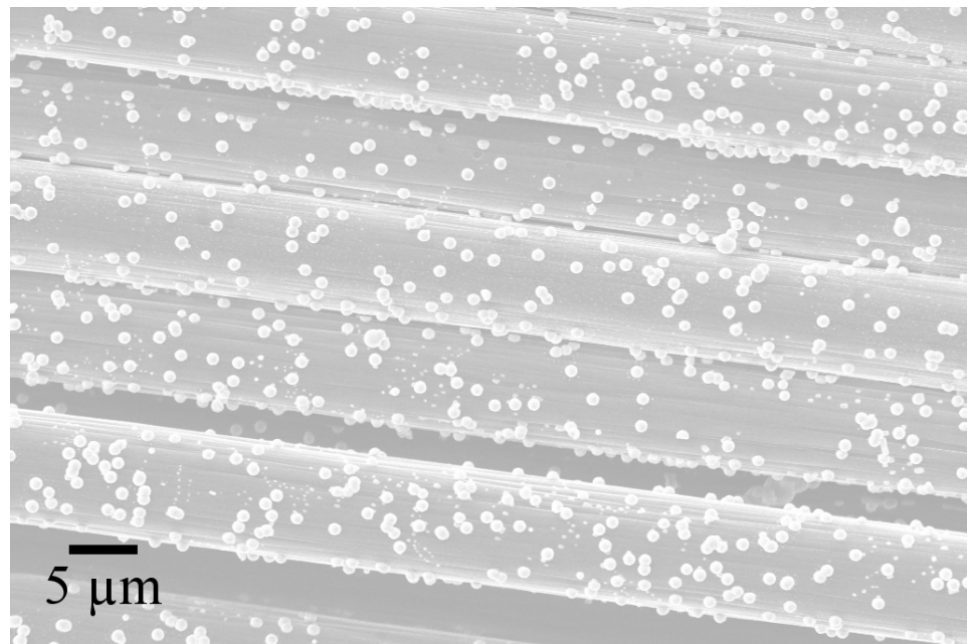


Fig. S3. EDS spectra of oxidized, nickel-coated UCFs.

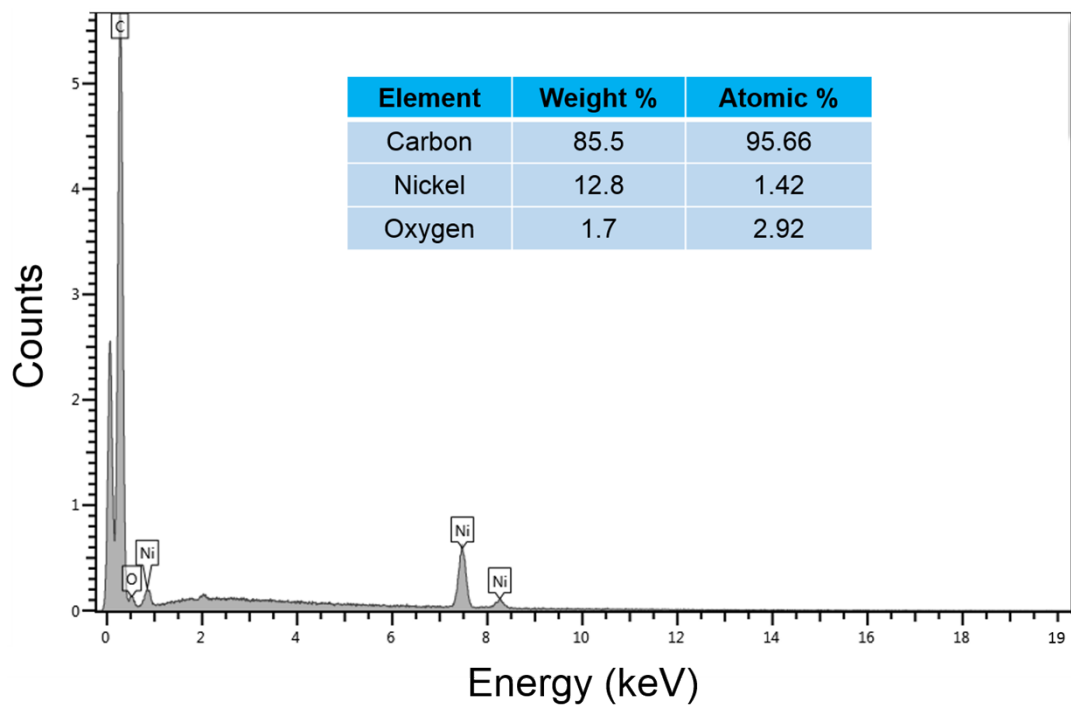


Fig. S4. Plot of variations in the volumetric capacitance of CNPs/UCF supercapacitor cell at different current densities.

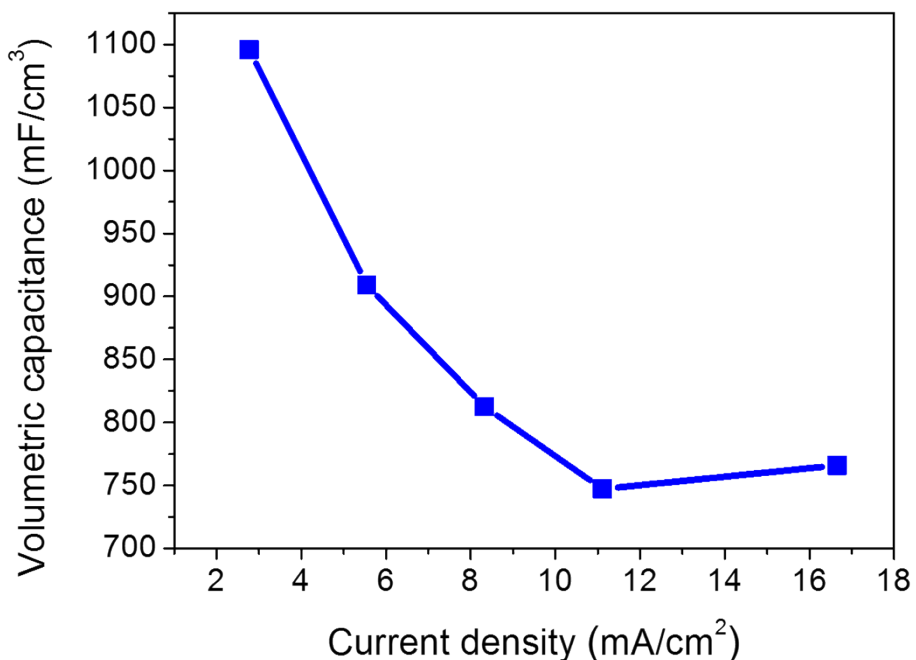


Fig. S5. Digital image of the two electrode cell set-up used for the testing of CNPs/UCF supercapacitor at various bending angles.

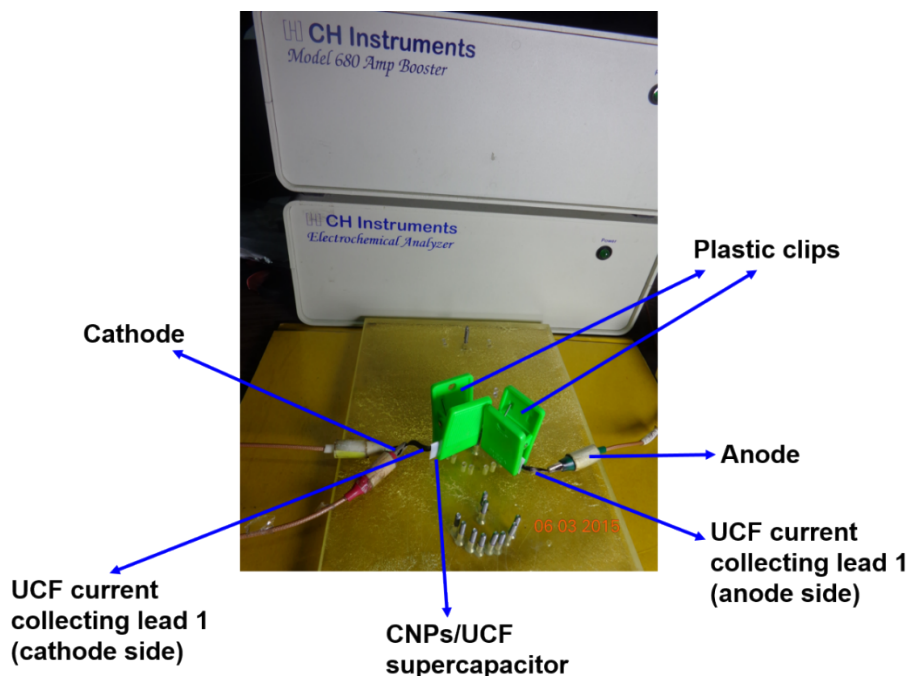


Fig. S6. Plot of percentage retention in the areal capacitance of CNPs/UCF supercapacitor cell at different bending angles.

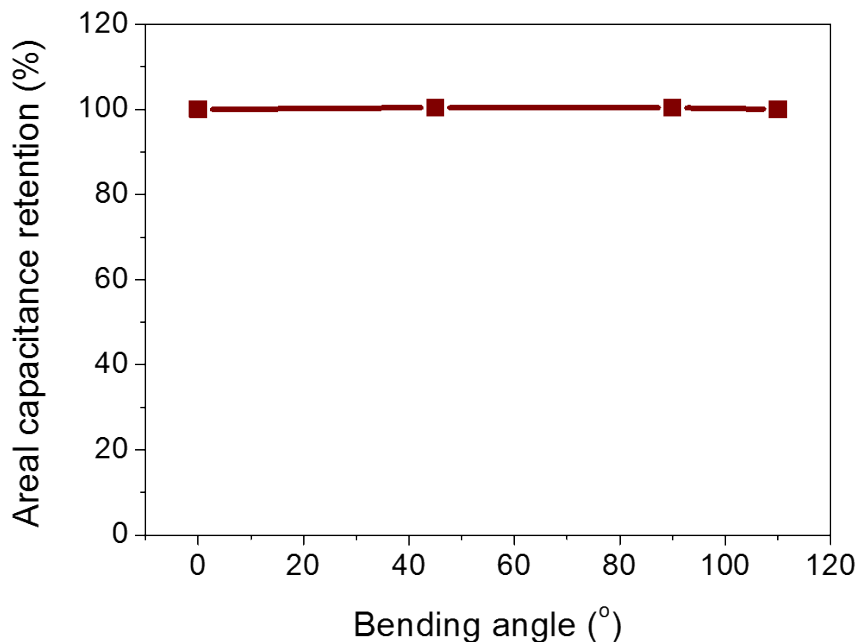


Fig. S7. Plot of percentage retention in the gravimetric capacitance of CNPs/UCF supercapacitor cell at different bending angles.

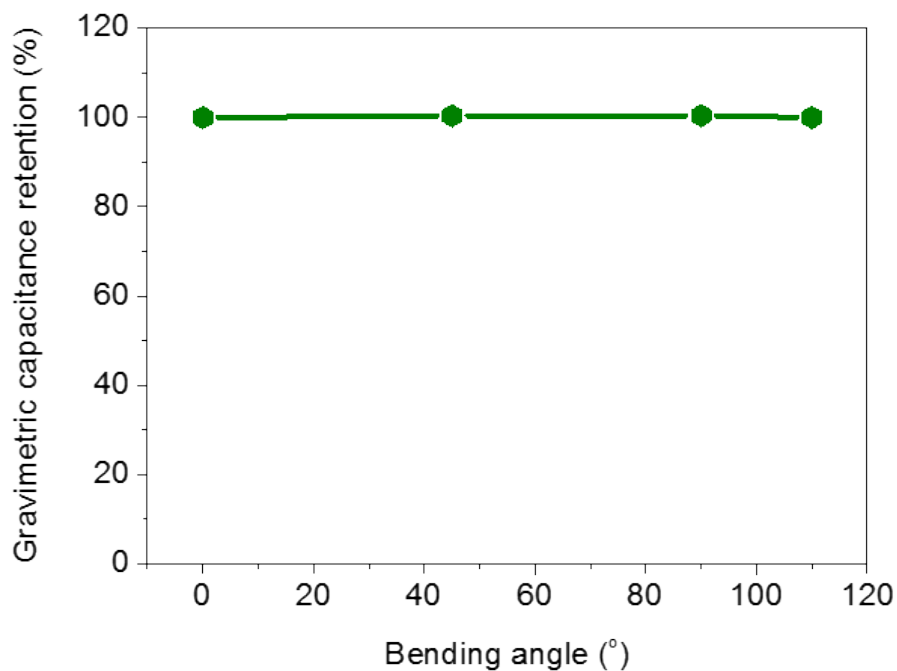


Fig. S8. Plot of variation in the volumetric capacitance of CNPs/UCF supercapacitor cell at different bending angles.

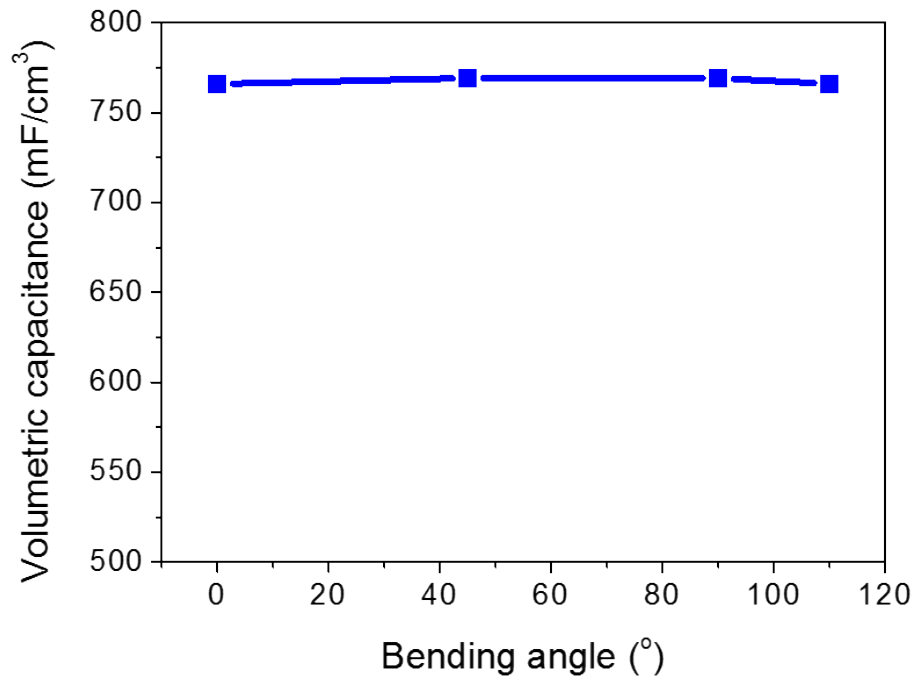


Fig. S9. Plots of percentage retentions in the volumetric and volume specific capacitances of CNPs/UCF supercapacitor cell at different bending angles.

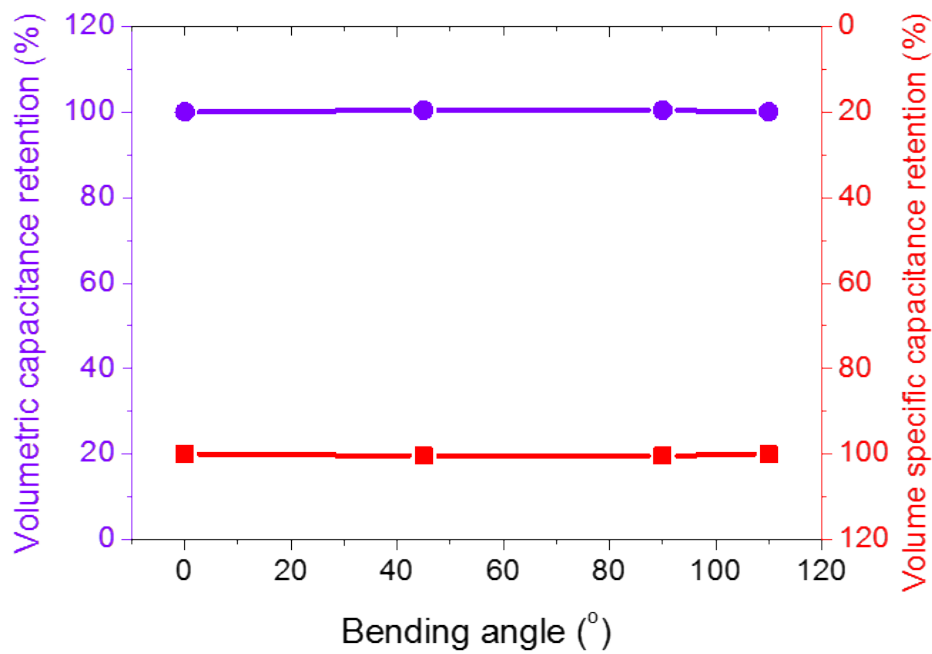


Fig. S10. Plot of variation in the gravimetric energy density of CNPs/UCF supercapacitor cell at different bending angles.

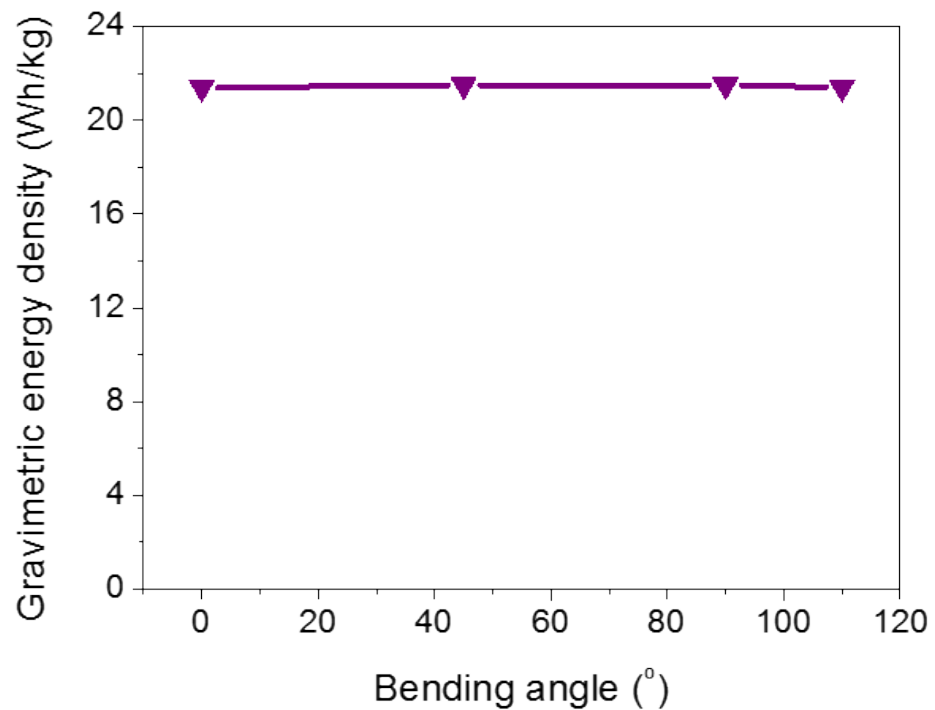


Fig. S11. Plots of percentage retentions in the volume specific and gravimetric energy densities of CNPs/UCF supercapacitor cell at different bending angles.

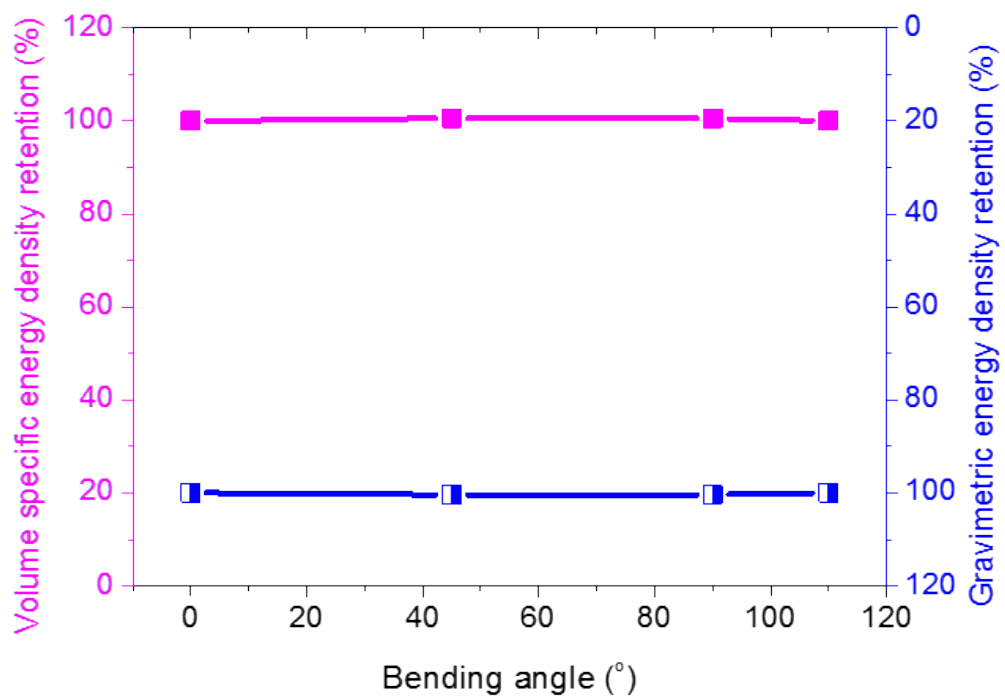
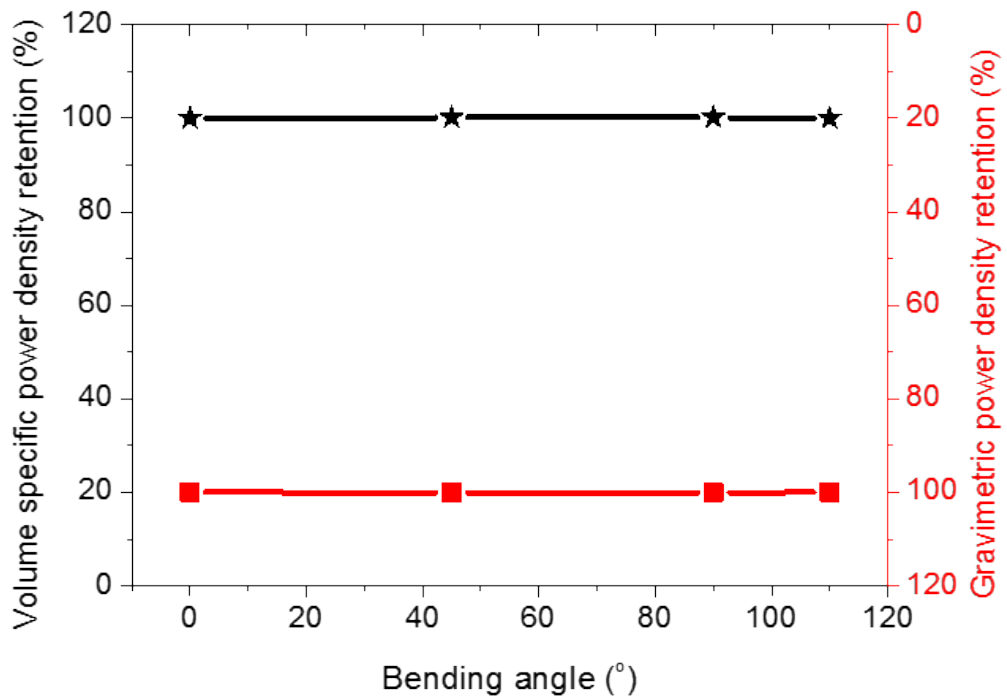


Fig. S12. Plots of percentage retentions in the volume specific and gravimetric power densities of CNPs/UCF supercapacitor cell at different bending angles.



References:

- [S1] D. Yu, K. Goh, H. Wang, L. Wei, W. Jiang, Q. Zhang, L. Dai, and Y. Chen, *Nature Nanotechnol.*, 2014, 9, 555.
- [S2] A. A. Zakhidov, D. S. Suh, A. A. Kuznetsov, J. N. Barisci, E. Munoz, A. B. Dalton, S. Collins, V. H. Ebron, M. Zhang, J. P. Ferraris, A. A. Zakhidov, and R. H. Baughman, *Adv. Funct. Mater.*, 2009, 19, 2266.
- [S3] E. Frackowiak, S. Gautier, H. Gaucher, S. Bonnamv, and F. Beguin, *Carbon*, 1999, 37, 61.
- [S4] Q. Jiang, M. Z. Qu, G. M. Zhou, B. L. Zhang, and Z. L. Yu, *Mater. Lett.*, 2002, 57, 988.
- [S5] C. S. Li, D. Z. Wang, T. X. Liang, G. T. Li, X. F. Wang, M. S. Cao, and J. Liang, *Sci. China, Ser. E-Technol. Sci.*, 2003, 46, 349.
- [S6] C. Du and N. Pan, *Nanotechnology*, 2006, 17, 5314.
- [S7] H. Mi, X. Zhang, S. An, X. Ye, and S. Yang, *Electrochem. Commun.*, 2007, 9, 2859.

- [S8] E. Frackowiak, K. Jurewicz, S. Delpeux, and F. Beguin, *J. Power Sources*, 2001, 97-98, 822.
- [S9] I. Y. Jang, H. Ogata, K. C. Park, S. H. Lee, J. S. Park, Y. C. Jung, Y. J. Kim, Y. A. Kim, and M. Endo, *J. Phys. Chem. Lett.*, 2010, 1, 2099.
- [S10] I. Y. Jang, H. Muramatsu, K. C. Park, Y. J. Kim, and M. Endo, *Electrochim. Commun.*, 2009, 11, 719.
- [S11] R. Shah, X. Zhang, and S. Talapatra, *Nanotechnology*, 2009, 20, 395202.
- [S12] R. Shi, L. Jiang, and C. Pan, *Soft Nanoscience Letters*, 2011, 1, 11.
- [S13] Z. Niu, W. Zhou, J. Chen, G. Feng, H. Li, W. Ma, J. Li, H. Dong, Y. Ren, D. Zhao, S. Xie, *Energy Environ. Sci.*, 2011, 4, 1440.
- [S14] C. Niu, E. K. Sichel, R. Hoch, D. Moy, H. Tennent, *Appl. Phys. Lett.*, 1997, 70, 1480.
- [S15] K. H. An, W. S. Kim, Y. S. Park, Y. C. Choi, S. M. Lee, D. C. Chung, D. J. Bae, S. C. Lim and Y. H. Lee, *Adv. Mater.*, 2001, 13, 497.